

Soft Matter

Accepted Manuscript



This is an *Accepted Manuscript*, which has been through the Royal Society of Chemistry peer review process and has been accepted for publication.

Accepted Manuscripts are published online shortly after acceptance, before technical editing, formatting and proof reading. Using this free service, authors can make their results available to the community, in citable form, before we publish the edited article. We will replace this *Accepted Manuscript* with the edited and formatted *Advance Article* as soon as it is available.

You can find more information about *Accepted Manuscripts* in the [Information for Authors](#).

Please note that technical editing may introduce minor changes to the text and/or graphics, which may alter content. The journal's standard [Terms & Conditions](#) and the [Ethical guidelines](#) still apply. In no event shall the Royal Society of Chemistry be held responsible for any errors or omissions in this *Accepted Manuscript* or any consequences arising from the use of any information it contains.

Molecular dynamics test of the Hertz-Knudsen equation for evaporating liquids

Robert Holyst^{*a}, Marek Litniewski^a, Daniel Jakubczyk^b

Received (in XXX, XXX) Xth XXXXXXXXX 200X, Accepted Xth XXXXXXXXX 200X

First published on the web Xth XXXXXXXXX 200X

DOI: 10.1039/b000000x

The precise determination of evaporation flux from liquid surfaces gives control over evaporation-driven self assembly in soft matter systems. The Hertz-Knudsen (HK) equation is commonly used to predict evaporation flux. This equation states that the flux is proportional to the difference between the pressure in the system and the equilibrium pressure for liquid/vapor coexistence. We applied molecular dynamics (MD) simulations of one component Lennard-Jones (LJ) fluid to test the HK equation for a wide range of thermodynamic parameters covering more than one order of magnitude in the values of flux. The flux determined in the simulations was 3.6 times larger than that computed from the HK equation. However, the flux was constant over time while the pressures in the HK equation exhibited strong fluctuations during simulations. This observation suggests that the HK equation may not properly grasp the physical mechanism of evaporation. We discuss this issue in the context of momentum flux during evaporation and mechanical equilibrium in this process. Most probably the process of evaporation is driven by tiny difference between the liquid pressure and the gas pressure. This difference is equal to the momentum flux i.e. momentum carried by the molecules leaving the surface of the liquid during evaporation. The average velocity in the evaporation flux is very small (two to three orders of magnitude smaller than the typical velocity of LJ atoms). Therefore the distribution of velocities of LJ atoms does not deviate from the Maxwell-Boltzmann distribution, even in the interfacial region.

I. Introduction

Evaporation is a ubiquitous process in nature affecting global warming and the efficiency of car engines. Controlled evaporation is used to crystallize proteins to elucidate their structures and ultimately their functions. The evaporation of solvents in soft matter systems permits the control of self-assembly. A dilute sample of micellar or polymer solution can easily be driven into more condensed phases by evaporation of the solvent instead of cumbersome mixing of the highly condensed phase. One can thus trace the whole phase diagram in the search for new phases and structures. For example, Nie et al.¹ demonstrated the efficient incorporation of nanorods into block copolymer cylindrical micelles by solvent evaporation-driven self-assembly. Merlin et al.² used a dedicated microfluidic tool based on evaporation to observe the nucleation and growth of charge-stabilized colloidal crystals. Toolan et al.³ used a spin-coating technique and showed that the ordering process of colloidal particles depends crucially on the volatility of the solvent. During fast evaporation only disordered aggregates are formed, while slow evaporation leads to well ordered structures. Jakubczyk et al.⁴, Derkachov et al.⁵ and Kolwas et al.⁶ observed various surface (thermodynamic) states and surface phase transitions in a freely evaporating droplet of suspension. Niton et al.⁷ created an artificial motor by driving collective rotations of chiral liquid crystalline molecules in a monolayer at the water surface. The whole system acted as a nano-windmill and was powered by water evaporation. The control of evaporation flux in this experiment permitted the slowing down of the

rotations to 10^{-2} Hz, i.e. to a frequency 14 orders of magnitude smaller than for the rotation of a single molecule. All the experiments related to ordering in soft matter systems via solvent evaporation show that precise control over evaporation flux is crucial for evaporation-driven self assembly in soft matter systems.

Evaporation mass flux from the liquid surface is commonly calculated from the Hertz-Knudsen (HK) equation.⁷ The HK equation (as derived by Knudsen himself) follows from the kinetic theory of gases, via the formula giving the number of molecules hitting a surface in gas at equilibrium, per unit area and unit time. The direct determination of the number density, and above all, true energy/velocity distribution of evaporating molecules, is experimentally hardly feasible (compare experiments on cold atoms in traps^{8,9}). Thus, out of necessity, the HK equation must be expressed in terms of intensive thermodynamic properties. Pressure and temperature are used instead of number density and mean velocity, while the mass flux is usually expressed by means of the rate of change of mass or temperature of the sample. Thus, the testing of the HK equation encounters a convolution of issues: the correct setting of the problem at a molecular level and the correct transition from extensive to intensive variables. The test also encompasses the long-standing problem¹⁰ of whether the rate of the process can be described by a formula devised for an equilibrium state. Experimental results obtained for rarefied gases (low vacuum) are obscured by effects such as back scattering, the formation of a Knudsen layer, etc. On the other hand, testing the HK equation in a high vacuum practically

limits measurements to the properties of the sample itself (change of temperature and/or mass) – the measurement of dynamic pressure and the pseudo-temperature of escaping vapor seems unfeasible.

The HK equation expressed in intensive thermodynamic variables relates the mass flux j_{HK} (defined as the number of particles evaporating per unit of time from the unit area) to the pressure difference:

$$j_{HK} = \frac{(p_{liq} - p_{eq})}{\sqrt{2\pi m k_B T_{liq}}} \quad (1)$$

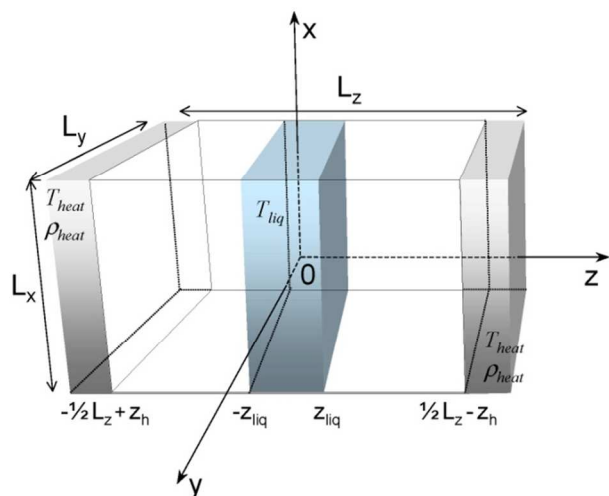


Fig.1 A schematic representation of a simulated system measuring $L_x \times L_y \times L_z$. In the middle of the system we place a liquid slab of thickness $2z_{liq}$ and temperature T_{liq} . At the beginning of the simulations the liquid slab is at equilibrium with its vapor at fixed temperature and pressure. The process of evaporation is initiated by heating the vapor far from the slab to a temperature T_{heat} higher than T_{liq} . The liquid temperature is not fixed, but settles during the evaporation process.

where p_{liq} is the pressure of the liquid during evaporation and p_{eq} is the equilibrium pressure of the vapor/liquid coexistence at T_{liq} – the temperature of the liquid during evaporation. Verification of the HK equation started with Knudsen himself. He became aware that the experimentally observed evaporation flux, j_m , was lower than that predicted theoretically, j_{HK} , and felt compelled to introduce a (notorious) evaporation coefficient α scaling the flux in Eq(1):

$$j_m = \alpha j_{HK} \quad (2)$$

Although there is no fundamental need for an evaporation coefficient α other than 1, the discussion of this issue recurs (just to mention a couple of reviews, spread over several decades).¹¹⁻¹⁶ However, it is admitted that the diversity of results, in particular those obtained for water¹¹⁻¹⁶ (α in the range from 0.001 to 1), seems to suggest that there may be some additional barrier for evaporation. *However, large variation of α cast doubt on the validity of the HK equation, if judged from the purely physical point of view.* Several decades after Knudsen, the problem of the evaporation coefficient still persists and often testing the HK equation is reduced to simply finding α .

The HK equation is routinely used in thermogravimetry¹⁷⁻¹⁹ (TG, TGA). In TG, the mass flux is monitored directly by weighting the sample under controlled temperature conditions. However, many TG experiments use a flow of neutral gas to carry evaporating molecules away and mimic vacuum evaporation. The corresponding evaporation coefficient has a different physical meaning than for ordinary evaporation into air. A review on evaporation of pure metals into a vacuum, mostly relying on TG experiments, is given in the paper by Safarian et al.¹⁵ The values of evaporation coefficients reported there are between 0.8 and 1. Interestingly, computer simulations²⁰ for argon evaporating into a vacuum gave $\alpha=2$ instead of 1. The computer simulations also revealed strong temperature profiles inside the evaporating liquid and thus cast doubts on the correct choice of temperature T_{liq} (Eq(1)) in the experiments. Further experiments of evaporation into a vacuum were performed by the Berkeley group²¹⁻²³. Their experiments were straightforward: droplets of water or other polar liquids were injected into a high vacuum (< 0.07 Pa). The temperature of the droplets was measured with Raman thermometry (with ± 2 K accuracy) versus the residence time²¹⁻²³. Since heat was carried away solely by evaporation, the evaporation flux could be determined. The mass loss and the temperature distribution inside the droplet were accounted for and the radiative heat transport was negligible. It was also noticed that the temperature dependence of the enthalpy of vaporization and of the heat capacity reciprocally cancelled out over the entire temperature range studied. Fitting the data to the HK equation required a temperature dependent evaporation coefficient. For example, the authors found the evaporation coefficient of water to be 0.6 ± 0.08 at 258 K. In determining the heat flux, the authors used a value of enthalpy of vaporization corresponding to the temperature equilibrium between phases (the values of enthalpy of vaporization are known along the vapor saturation line). This raises some old concerns, (recognized for example in the context of supersonic expansion²⁴) since evaporation into a vacuum is far from equilibrium in many respects. It can be argued¹⁹ that the equilibrium enthalpy of evaporation should be supplemented with the kinetic energy associated with the flux escaping ballistically into the vacuum (compare: stagnation versus static enthalpy). However, it can also be shown that the additional terms in the enthalpy are below 20% of the whole enthalpy and can hardly be responsible for the whole discrepancy of the obtained value of evaporation coefficient versus the results of other authors. The Boston College/Aerodyne Research group was able to verify the HK equation at equilibrium.²⁵ In this case, a train of droplets of water was travelling in an atmosphere at full equilibrium with them, which resulted in no overall mass exchange. However, isotopic labelling was used to count interchanged particles (natural gas/liquid isotope partitioning was accounted for) and the result was compared with the HK equation prediction. The value of the evaporation coefficient for water obtained by the Boston College/Aerodyne Research²⁵ group in the same

temperature range as the Berkeley group used²¹⁻²³ (~258 K) was 0.32 ± 0.04 . Their results are in agreement with those of the IP/IPC PAS group obtained (indirectly) from the HK equation relatively close to equilibrium.²⁶ The IP/IPC PAS group studied the evaporation of single levitated droplets of water in nearly saturated vapor. In general, different measurements/computer simulations performed by different techniques and groups show²⁷ that the evaporation coefficient α in Eq(2) is between 0.001 and 2. Even the most precise experiments²¹⁻²⁷ differ by a factor of 2 and the discrepancy between experiments and computer simulations is almost one order of magnitude as we show in this paper. Such huge differences indicate that Eqs(1-2) may not correctly grasp the physical mechanism behind the evaporation process. The purpose of this paper is to test the the HK equation in situations more common to evaporation-assisted self assembly i.e. at high vapor pressure. We show that $\alpha=3.6$ in this case. Thus the discrepancy between experiments (Boston group^{25,28} $\alpha=0.3$) and our computer simulations ($\alpha=3.6$) is one order of magnitude. We identified two problems in such tests (either experimental or in computer simulations). One of them is the precise determination of the equilibrium pressure. Because evaporation is driven by very small pressure differences, a small relative error in this quantity precludes proper verification of the HK equation. For this reason, a precise test of Eqs.(1-2) requires very precise determination of the phase diagram and the pressures. The second problem is the flow around the evaporating droplet which changes the mechanical equilibrium and affects the mass flux from the evaporating surface. We discuss both issues in our paper. The paper is organized as follows: In section 2 we define the system. In section III we analyze the evaporation of the liquid slab and test the HK equation. Section IV contains our conclusions and further analysis based on the momentum flux and mechanical equilibrium established in the system during evaporation.

II. Computer simulations – description of the system

The simulations were performed using the classical molecular dynamic (MD) method. Periodic boundary conditions were applied in the simulation box. In order to attain the desired level of accuracy (see Supporting Information), Newton equations of motion were solved using the Cowell-Numerov 4-th order implicit method^{29,30}. The fluid consisted of Lennard-Jones (LJ) particles interacted by the potential truncated at $R = 2.5\sigma$ in a following way:

$$\varphi(r) = \begin{cases} \varepsilon \left(\left(\frac{\sigma}{r} \right)^{12} - \left(\frac{\sigma}{r} \right)^6 \right) + \delta & \text{for } r/\sigma \leq 2 \\ \gamma \left(\frac{r}{\sigma} - R \right)^2 \Theta \left(R - \frac{r}{\sigma} \right) & \text{for } 2 < r/\sigma \end{cases} \quad (3)$$

where r is the inter-particle distance, Θ is the Heaviside function, ε and σ are the particle energy and size; γ and δ are the constants adjusted to make $\varphi(r)$ differentiable in the whole space. All the numerical values given further on are expressed in

reduced LJ units. For argon the values of the units are: length ($\sigma = 3.5 \times 10^{-10}$ m), number density ($2.33 \times 10^{28} \text{ m}^{-3}$), mass ($m = 40 \text{ amu}$), time ($\sigma(m/\varepsilon)^{1/2} = 2.3 \text{ ps}$), energy ($\varepsilon = 112 k_B \text{ K} = 1.5 \times 10^{-21} \text{ kg m}^2/\text{s}^2$ and $\varepsilon/k_B = 112 \text{ K}$ sets the temperature scale), velocity (150 m/s), momentum (10^{-23} kg m/s), pressure ($3.6 \times 10^6 \text{ kg}/(\text{m} \times \text{s}^2)$).

The simulated system is shown in Fig. 1. The simulations were performed using a constant energy and volume method in a box with edges $L_x = L_y \approx 80 \rho_{\text{liq}}^{-1/3}$, where ρ_{liq} is the liquid density. L_z/σ changed from 704 to 1468 depending on the gas density. The total initial number of particles at liquid state was always 448,000 and at the gas state varied from 182,016 to 359,370. The mass center of the liquid slab was always placed in the center of the whole system and periodic boundary conditions were applied along all axes. We defined the liquid surface as the xy surface crossing the z axis at $z = \pm z_{\text{liq}}$, where the local density is equal to one-half of its maximum value. The liquid parameters: T_{liq} , ρ_{liq} , p_{liq} were determined by averaging over all the particles placed at least 10σ below z_{liq} . Boundary conditions that forced evaporation were applied at the ends of the z axis (Fig.1) by introducing subsystems at $z > 0.5L_z - z_h$ and $z < -0.5L_z + z_h$ where z_h had a value between 40σ and 75σ depending on the gas density and the system size. The temperature of the subsystem was kept constant (by scaling the velocities) and equal to the heating temperature T_{heat} significantly larger than T_{liq} . The pressure was controlled by keeping the subsystem (Fig.1) density lower than the density ρ_{heat} . The condition was realized by randomly removing particles from the subsystem. Both velocity scaling and particle removal were performed once every 20 time steps. The procedure did not change the subsystem momentum - the total momentum of the system was always equal to 0. The accuracy of our simulations and the sources of errors are presented in the Supporting Information.

All simulation values of the temperature and pressure were calculated from the standard formulas involving z -th components of velocity and the z component of the pressure tensor:

$$T = \frac{\sum_{j=1}^n v_{zj}^2}{nk_B} \quad (4)$$

$$p = p_{zz} = \frac{1}{V} \left(\sum_{j=1}^n \left(mv_{zj}^2 - \sum_{i>j}^n z_{ij} \frac{\partial \varphi}{\partial z_{ij}} z_{ij} \right) \right) \quad (5)$$

V is the volume enclosing n particles, v_{zj} is the z -component of the velocity of j particle, n is the number of particles and z_{ij} is the z -component of the vector joining the center of mass of particles i and j . The equipartition rule held in all the cases considered. Due to the small system size, the fluctuations and, as a result, the errors of T and especially of p estimated using the z -component of velocity and pressure tensor were significantly lower than those for the calculations using the x or y components. The temperature of the liquid varied between 0.797 and 0.899 (Table S1 in the Supporting Information) and the equilibrium pressure varied between

0.014 and 0.032 (with a typical error of 10^{-5} , see Table S1 Supporting Information). Eq(4) is valid for temperature determination, because the z-component velocity distribution in the interfacial region and also in the gas and liquid phase is practically given by the Maxwell-Boltzmann function (Supporting Information).

III. Results: average mass flux and mass flux as a function of time

The difference between the vapor or liquid pressure and the vapor-liquid equilibrium value $p_{eq}(T)$ is very small during evaporation. Therefore the study requires computer simulations at a very high level of accuracy. For the LJ vapor liquid equilibrium the literature gives $p_{eq}(T)$ with an error of around $1-2 \times 10^{-4}$ in LJ units, which is much too high for our purpose of testing the HK equation. We found sufficiently accurate $p_{eq}(T)$ data (with errors of around 10^{-5} to 5×10^{-6}) by performing our own vapor-liquid equilibrium simulations for two phase systems described by potential given by Eq(3). Both equilibrium and non-equilibrium (evaporation) simulations were performed for systems of very similar sizes to eliminate the possible influence of a finite system size (the so called size effect) on the difference between p and p_{eq} . The results are given in Table S1 (Supporting Information). The values of the equilibrium pressure obtained in the simulations (Table S1 in the Supporting Information) were fitted with the equation³¹ (Antoine equation) (6):

$$p_{eq}(T) = A \exp\left(-\frac{B}{T+C}\right) \quad (6)$$

with the following values of the parameters: $A=26.6913$, $B=6.21423$, $C=0.025386$. The standard error for the pressure from Eq(6), $\sigma_e \sim 10^{-5}$, was estimated on the basis of the data from Table S1. In further analysis the vapor-liquid equilibrium pressure $p_{eq}(T)$ was calculated from Eq(6). The non-equilibrium simulations started from the initial conditions of the equilibrium between the liquid slab and the vapor (Fig. 1; Table S1 Supporting Information). We initiated evaporation by heating the gas phase subsystem (Fig.1) well above z_{liq} to T_{heat} and changed its density to ρ_{heat} (Table S2 Supporting Information). The temperature of the subsystem remained equal to T_{heat} during the whole evaporation process (Fig.1). After the strongly non-equilibrium behavior of the system at the beginning of the evaporation process the system attained a quasi-stationary regime during which the liquid thermodynamic parameters were approximately constant. The temperature, density and pressure profiles are shown in Fig. S1 in the Supporting Information. The system develops a temperature profile in the quasi-stationary regime and evaporates at the expense of the internal energy of the gas phase – we add the energy in the subsystem shown in Fig. 1 by keeping its temperature constant at $T=T_{heat}$. The temperature changes linearly with distance z from T_{heat} at the border of the simulation box to T_{liq} at the surface of the liquid (Fig.S1 Supporting Information). The temperature is constant and equal to $T=T_{liq}$ in the whole liquid slab. The vapor density changes such that together with the temperature changes it ensures a

constant pressure in the vapor phase. Finally within the error of the simulations the pressure in the liquid is equal to the pressure of the vapor. We consider this issue of mechanical equilibrium during evaporation further in the discussion section. The results of non-equilibrium simulations are given in Table S2 in the Supporting Information and Fig.2.

The flux was measured directly using Eq.(7) in three regions, each restricted by 2 xy surfaces, shifted above z_{liq} by z_i and z_{i+1} where $z_i/\sigma = 5, 15, 25$ and 40 for $i = 1..4$.

$$j_m = \frac{1}{V} \langle \sum_{j=1}^n v_{z_j} \rangle \quad (7)$$

where the summation is over all n particles enclosed in the considered volume V and $\langle \rangle$ means the time averaging. In the steady state regime, the results were independent of the studied region along the z -axis. According to the generalization to the Hertz-Knudsen relation, the flux from liquid to gas during evaporation is given by Eq.(2). The estimation for the evaporation coefficient α was found by using the parameters from Table S2 (Supporting Information) in the minimization of

$$W^2 = \frac{(j_m - j_{HK})^2}{\sigma_e(j_{HK})^2} \quad (8)$$

From this procedure we obtain $\alpha = 3.6 \pm 0.4$. $\sigma_e(j_{HK})$ in (8) estimates the standard error.

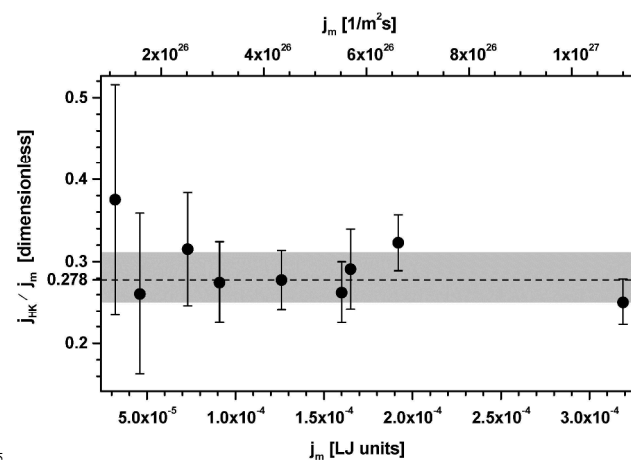


Fig.2 The ratio j_{HK}/j_m (filled circles) as a function of j_m . The error bars are $\sigma_e(j_{HK})/j_m$ (Table S2). The dashed line and the grey band represent α^{-1} and its error respectively. The data are from Table S2 in the Supporting Information.

The fluxes presented in Fig. 2 were averaged over time during the whole evaporation process in a quasi-stationary regime. No dependence of the ratio j_{HK}/j_m on j_m can be seen. However for small j_m the errors are very high. This is an important argument for the validity of the estimation for α since any non-physical effect, if present, should influence the pressure difference in Eq.(1) relatively much more strongly for small j_{HK} than for larger values. In Fig. 3 we show the flux as a function of time together with the HK flux predicted from Eq.(1). Interestingly, although j_m is nearly constant during the simulations, the pressure difference (in the HK equation Eq(1)) strongly fluctuates and the time-scale of fluctuations is very large. This sort of behavior was

characteristic for all non-equilibrium simulations from Table S2 and Fig.S2 in the Supporting Information.

IV. Conclusions and new hypothesis concerning evaporation

Fig. 3 gives direct proof that mass flux from the surface of a liquid is not **directly** driven by the difference between the liquid pressure and the equilibrium pressure. The mass flux divided by the evaporation coefficient $\alpha^1 j_m$ (Eq(5)) is constant and equal to around 4×10^{-5} after reaching the stationary state (at times larger than 16 000 units). But, the flux, j_{HK} , determined from the pressure difference fluctuates between 8×10^{-5} and 2×10^{-5} . Such large changes of j_{HK} and almost constant flux, j_m , suggest that the mechanism of evaporation is not properly grasped by the HK equation (Eq(1)). In all studied cases (for various thermodynamic conditions) we observed very large fluctuations of j_{HK} and nearly constant flux, j_m (Supporting Information). Here we will put forward a hypothesis as to the possible mechanism of evaporation and notorious problems in experimental/computer simulation tests of the HK equation.

20

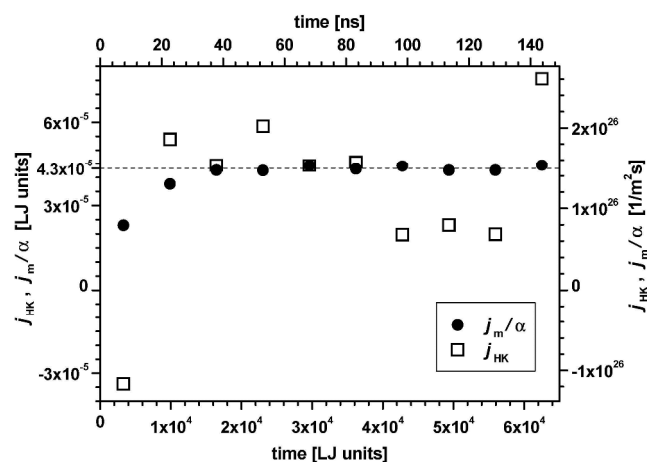


Fig.3 Fluxes j_{HK} (empty squares) and $\alpha^1 j_m$ (black circles) as a function of time for simulation at the following thermodynamic conditions ($p_{liq} = 0.02273$, $T_{liq} = 0.85323$, $\rho_{heat} = 0.0115$, $T_{heat} = 2.0$). Each point is averaged over a time interval of 6580 LJ units length during which around 17,000 particles evaporated from both sides of the liquid slab. The liquid surface parameter z_{liq} decreased during the interval by around 1.5σ . The first two points are obtained in the initial non-stationary stage.

In our previous publication²⁰ we observed that a liquid slab evaporating into a vacuum is characterized by the following equation:

$$p_{liq} = j_p \quad (9)$$

where p_{liq} is the pressure inside the liquid slab and j_p is the momentum flux from the surface. The momentum carried by particles leaving the surface of the liquid compensates the pressure inside the liquid. Thus the evaporation process is like shooting a cannon, where the shell and cannon jointly keep the momentum equal to 0 in the shot. The momentum flux is given by

$$j_p = \frac{1}{2} m \rho_{ev} u^2 \quad (10)$$

where ρ_{ev} is the number density in the evaporating flux, m is the mass of the molecule and u is the average velocity in this flux. The mass flux is given by

$$j_m = m \rho_{ev} u \quad (11)$$

From Eqs (10-11) we find that the relation between the liquid pressure and the mass flux is:

$$j_m = \sqrt{2m\rho_{ev}p_{liq}} \quad (12)$$

or

$$j_m = \sqrt{\frac{2mp_{liq}}{u}} \quad (13)$$

We think that this equation may be generalized to other cases i.e. evaporation into vapor of non-zero pressure i.e.

$$p_{liq} - p_{vap} = j_p \quad (14)$$

where the difference between liquid and vapor pressures during evaporation is exactly matched by the momentum flux from the surface of the evaporating liquid. Equation (14) has a natural limit of evaporation into a vacuum ($p_{vap}=0$), given by Eq(9), which has been verified in many simulations.^{20,32} Unfortunately, at high vapor pressure, studied in this paper, this equation is extremely hard to test because all the pressure differences, evaporation density and velocity u are very small. For example, in our simulations the largest evaporation flux $j_m=3.2 \times 10^{-4}$ LJ units, where one LJ flux unit is $3.5 \times 10^{30}/(m^2s)$. Because the typical density in this case is between $\rho_{ev}=0.01$ and 0.04 and the velocity is between $u=0.008$ and 0.032 , we find that the momentum flux and the pressure difference in Eq(14) are in the order of 10^{-5} to 10^{-6} in LJ units. These momentum fluxes are comparable or even smaller than the errors in the pressure determination. The smallest mass fluxes determined in our simulations ($\sim 10^{-5}$) and typical velocities for this flux are of the order of 10^{-3} i.e. 0.15 m/s. Thus the pressure difference in Eq.(14) is 10^{-8} in this case, whereas the accuracy in the determination of the pressure is 10^{-5} (three orders of magnitude larger). In experiments the tests are even harder, because the experimental fluxes are orders of magnitude smaller than the ones obtained in our simulations. In our units they are between 10^{-7} and 10^{-11} . For example, for a water droplet evaporating down to $0.8 \mu m$ in radius, in air at atmospheric pressure at 286.8 K and ~ 0.97 relative humidity, the flux does not exceed $1.4 \times 10^{23}/(m^2s)$ which is 10^4 times smaller than in the presented simulation. For a similar droplet of diethylene glycol evaporating in dry nitrogen (a void of glycol vapor) at 298 K the flux is a further 100 times smaller i.e. $10^{21}/(m^2s)$. Such small fluxes correspond to very small mean velocities, u , much smaller than cm/s. This means that if an evaporating droplet of micrometer size moves at even a small velocity (even mm/s) its momentum is sufficient to modify the momentum flux during evaporation and therefore to significantly change the mass flux. Maybe this is the main reason for the large divergence of evaporation coefficients found in experiments and computer simulations. In most experiments the

vapor moves with respect to the evaporating liquid surface and therefore affects the mechanical equilibrium set by Eq.(14), changing the mass flux accordingly. The analysis of the average velocity in the flux suggests that for practical reasons the Maxwell-Boltzmann distribution is valid for the z-component of the velocity as illustrated in the Supporting Information (Fig.S4).

Summarizing: our results suggest (Fig.3) that the Hertz-Knudsen equation does not correctly describe the evaporation process. We put forward a hypothesis that evaporation is driven by tiny differences between pressure in the evaporating liquid phase and pressure in the vapor phase. The momentum flux of evaporating molecules/atoms should exactly balance this difference during evaporation. We further hypothesize that the density ρ_{ev} in the evaporation flux is probably equal to the density of the vapor at equilibrium with a liquid at temperature T_{liq} . More careful experiments at reduced pressure of the vapor at rest or at controlled flow conditions are needed to investigate this problem further. Computer simulations performed in vacuum conditions are a good starting point for such investigations.

Finally, the self-assembly process via controlled evaporation is currently a very promising way to build large scale hierarchical structures in soft matter systems³³⁻³⁶. New methods for controlling this process based on pressure variations and flow can emerge from our theoretical study, especially when combined with novel sophisticated experiments³⁷ performed in evaporating systems.

Acknowledgement: This work was supported by the National Science Center, Poland under grant number 2014/13/B/ST3/04414.

Notes and references

^a Institute of Physical Chemistry Polish Academy of Sciences, Kasprzaka 44/52,01-224 Warsaw, Poland rhoyst@ichf.edu.pl mlitniewski@ichf.edu.pl

^b Institute of Physics of the Polish Academy of Sciences, Al Lotnikow 32-46, PL-02668, Warsaw, Poland

† Electronic Supplementary Information (ESI) available: [details of MD simulations].

- 1 X. Nie, J. Cui and W. Jiang *Soft Matter* 2014, **10** 8051.
- 2 A. Merlin, J.-B. Salmon, and J. Leng *Soft Matter* 2012, **8**, 3526.
- 3 D.T.W. Toolan, S.Fujii, S.J.Ebbens, Y.Nakamura, J.R.Howse *Soft Matter* 2014, **10**, 8804.
- 4 D. Jakubczyk, M. Kolwas, G. Derkachov, K. Kolwas, *J. Phys. Chem. C*, 2009, **113**, 10598.
- 5 G. Derkachov, K. Kolwas, D. Jakubczyk, M. Zientara, and M. Kolwas, *J. Phys. Chem. C*, 2008, **112**, 16919.
- 6 M. Kolwas, K. Kolwas, G. Derkachov, D. Jakubczyk, *Phys. Chem. Chem. Phys.*, 2015, **17**, 6881.
- 7 P.Niton, A.Zywocinski, A.Fialkowski and R.Holyst, *Nanoscale* 2013, **5**, 9732.
- 8 W.Ketterle, M.W.Zwierlein Proc. Int. School of Physics Enrico Fermi, IOS, Amserdam 2006.
- 9 C. Sabin, A. White, L. Hackermuller and I. Fuentes, *Sci. Rep.*, 2014, **4**, 6436.
- 10 K. C. D. Hickman, *Industrial & Engineering Chemistry* 1954, **46**, 1442.
- 11 G.M. Pound, *J. Phys. Chem. Ref. Data*, 1972, **1**, 135.
- 12 R. Marek and J. Straub, *Int. J. Heat Mass Transfer* 2001, **44**, 39.
- 13 L.W. Eames, N.J. Marr and H. Sabir, *Int. J. Heat and Mass Transfer* 1997, **40**, 4522.
- 14 E.J. Davis, *Atmos. Res.* 2006, **82**, 561.

- 15 J. Safarian and A.E. Thorvald, *Metallurgical and Materials Transactions A*, 2013, **44A**, 2013, 747.
- 16 C.E. Kolb et al., *Atmos. Chem. Phys.*, 2010, **10**, 10561.
- 17 D.M. Price, *J. Therm. Anal. Cal.*, 2001, **64**, 315.
- 18 A. Auroux, *Calorimetry and Thermal Methods in Catalysis*, Springer Series in Materials Science, 2013, Springer.
- 19 C.T. Ewing, K.H. Stern, *J. Phys. Chem.*, 1975, **79**, 2007.
- 20 R.Holyst and M.Litniewski, *J.Chem.Phys.* 2009, **130**, 074707.
- 21 K.R. Wilson, B.S. Rude, J.D. Smith, C.D. Cappa, D.T. Co, R.D. Schaller, M. Larsson, T. Catalano, R.J. Saykally, *Rev. Sci. Inst.*, 2004, **75**, 725.
- 22 J.D. Smith, C.D. Cappa, W.S. Drisdell, R.C. Cohen, and R.J. Saykally, *J. Am. Chem. Soc.*, 2006, **128**, 12892.
- 23 Duffey et al., *Phys. Chem. Chem. Phys.*, 2013, **15**, 11634.
- 24 W. Christen and K. Rademann, *Phys. Scr.*, 2009, **80**, 048127.
- 25 Y.Q. Li, H.Z. Zhang, P. Davidovits, J.T. Jayne, C.E. Kolb, D.R. Worsnop, *J. Phys. Chem. A*, 2002, **106**, 1220.
- 26 M. Zientara, D. Jakubczyk, K. Kolwas, M. Kolwas, *J. Phys. Chem. A*, 2008, **112**, 5152.
- 27 R. Holyst, M. Litniewski, D. Jakubczyk, K. Kolwas, M. Kolwas, K.Kowalski, S. Migacz, S. Palesa, M. Zientara, *Rep. Prog. Phys.*, 2013, **76**, 034601.
- 28 Y. Li, P. Davidovits, Q. Shi, J. Jayne, C. Kolb, D.J. Worsnop, *J Phys. Chem. A*, 2001, **105**, 10627.
- 29 M. Litniewski, *Mol. Simul.* 2003, **29**, 223.
- 30 R. D. Skeel, G. Zhang, and T. Schlick, *SIAM J. Sci. Comput.* 1997, **18**, 203.
- 31 R. C. Reid, J. M. Prausnitz, B. E. Poling, *The Properties of Gases and Liquids* (McGraw-Hill, New York, 1988).
- 32 S.Cheng et al. *J.Chem.Phys* 2011, **134**, 224704.
- 33 W.Han et al. *Angew. Chem.Int.Ed.* 2013, **52**, 2564-2568.
- 34 M.Byun et al, *Angew. Chem.Int.Ed.* 2013, **52**,1122-1127.
- 35 B.Li et al, *ACS Nano* 2014, **8**, 2936-2942.
- 36 B.Li et al, *Angew. Chem.Int.Ed.* 2015, **54**,4250-4254.
- 37 S. Dehaeck, A. Rednikov, P.Colinet, *Langmuir.*, 2014, **30**, 2002-2008

